



TITLE:

Chronic reduction of GIP secretion alleviates obesity and insulin resistance under high fat diet condition(Dissertation_全文)

AUTHOR(S):

Nasteska, Daniela

CITATION:

Nasteska, Daniela. Chronic reduction of GIP secretion alleviates obesity and insulin resistance under high fat diet condition. 京都大学, 2014, 博士(医学)

ISSUE DATE:

2014-07-23

URL:

<https://doi.org/10.14989/doctor.k18501>

RIGHT:

This dissertation is author version of following the journal article. Daniela Nasteska, Norio Harada, Kazuyo Suzuki, Shunsuke Yamane, Akihiro Hamasaki, Erina Joo, Kanako Iwasaki, Kimitaka Shibue, Takanari Harada, and Nobuya Inagaki. Chronic Reduction of GIP Secretion Alleviates Obesity and Insulin Resistance Under High-Fat Diet Conditions. Diabetes July 2014 63:7 2332-2343; published ahead of print February 28, 2014, doi:10.2337/db13-1563 1939-327X

Chronic reduction of GIP secretion alleviates obesity and insulin resistance under high fat diet
condition

Running title: GIP reduction alleviates obesity

Daniela Nasteska¹, Norio Harada¹, Kazuyo Suzuki¹, Shunsuke Yamane¹, Akihiro Hamasaki¹,
Erina Joo¹, Kanako Iwasaki¹, Kimitaka Shibue¹, Takanari Harada¹, Nobuya Inagaki¹

¹Department of Diabetes, Endocrinology and Nutrition, Graduate School of Medicine, Kyoto
University, Kyoto, Japan

Corresponding author: Nobuya Inagaki, Department of Diabetes, Endocrinology and Nutrition,
Graduate School of Medicine, Kyoto University, 54 Kawahara-cho, Shogoin, Sakyo-ku, Kyoto
606-8507, Japan. Tel: +81 75 751 3562, fax: +81 75 771 6601, e-mail:

inagaki@metab.kuhp.kyoto-u.ac.jp

Abstract word count: 195

Main text word count: 4984

Tables: 1

Figures: 5

Supplementary figures: 1

Abstract:

Gastric inhibitory polypeptide (GIP) exhibits potent insulinotropic effects on β -cells and anabolic effects on bone formation and fat accumulation. We explored the impact of reduced GIP levels *in vivo* on glucose homeostasis, bone formation, and fat accumulation in a novel GIP-GFP knock-in (KI) mouse. We generated GIP-GFP KI mice with a truncated *prepro-GIP* gene. The phenotype was assessed in heterozygous and homozygous state in mice on control fat diet (CFD) and high fat diet (HFD) *in vivo* and *in vitro*. Heterozygous GIP-GFP KI mice (GIP-reduced mice: $\text{GIP}^{\text{gfp}/+}$) exhibited reduced GIP secretion; in homozygous state (GIP-lacking mice: $\text{GIP}^{\text{gfp}/\text{gfp}}$), GIP secretion was undetectable. When fed standard chow, $\text{GIP}^{\text{gfp}/+}$ and $\text{GIP}^{\text{gfp}/\text{gfp}}$ showed mild glucose intolerance with decreased insulin levels; bone volume was decreased in $\text{GIP}^{\text{gfp}/\text{gfp}}$ and preserved in $\text{GIP}^{\text{gfp}/+}$. Under HFD, glucose levels during OGTT were similar in WT, $\text{GIP}^{\text{gfp}/+}$, and $\text{GIP}^{\text{gfp}/\text{gfp}}$, while insulin secretion remained lower. $\text{GIP}^{\text{gfp}/+}$ and $\text{GIP}^{\text{gfp}/\text{gfp}}$ showed reduced obesity and reduced insulin resistance, accompanied by higher fat oxidation and energy expenditure. GIP-reduced mice demonstrate that partial reduction of GIP does not alter extensively glucose tolerance, but it alleviates obesity and lessens the degree of insulin resistance under HFD condition, suggesting a potential therapeutic value.

Keywords: GIP, incretin, bone volume, obesity, insulin resistance

Abbreviations:

GIP gastric inhibitory polypeptide

GLP-1 glucagon-like polypeptide-1

GIPR GIP receptor

GIPRKO GIP receptor knockout

GIP-GFP KI gastric inhibitory polypeptide-green fluorescent protein knock-in

CFD control fat diet

HFD high fat diet

GIP^{gfp/+} heterozygous GIP-GFP KI

GIP^{gfp/gfp} homozygous GIP-GFP KI

Gastric inhibitory polypeptide (GIP) is a 42-amino acid polypeptide produced by enteroendocrine K-cells, which are located mainly in the upper parts of the small intestine. Its main secretagogues are glucose and, even more intensely, fats that reach the intestinal lumen soon after food intake (1). Following secretion, the hormone exerts its effects through specific, G protein-coupled receptors located mainly in the stomach, pancreas, central nervous system, bone and adipose tissue (2, 3). Apart from its role in the inhibition of gastric acid secretion (4), GIP exhibits potent glucose-dependent insulinotropic action (5, 6), and, therefore, it is classified as an incretin (3). In addition to its insulinotropic effect, in the absence of which glucose intolerance develops (7), GIP stimulates islet growth (8) and proliferation of β -cells (9) and reduces β -cell apoptosis (10, 11). Studies of GIP receptor knockout (GIPRKO) mice (7) describe GIP as an obesity-promoting factor in high fat diet (HFD) conditions, and show that deletion of GIP receptor (GIPR) signaling causes resistance to obesity (12) but leads to osteoporosis (13), revealing an important role of GIP in bone metabolism. However, in these studies, as well in a model of GIP receptor antagonism (14), the reported changes were focused on disrupted or blocked GIPR signaling. The condition of reduced GIP secretion and how it affects the pancreatic and extrapancreatic effects of GIP remain unclear.

The aim of the present study is to explore the potential of reduced GIP levels *in vivo* and to define the impact on glucose homeostasis, bone formation, and fat accumulation in a novel GIP-GFP knock-in (KI) mouse model characterized by truncation of the prepro-GIP gene and insertion of a Green Fluorescent Protein (GFP) sequence (15). The model was developed for the purpose of visualization and identification of K-cells, and exhibits reduced or absent GIP secretion in heterozygous GIP-reduced mice and homozygous or GIP-lacking mice, respectively.

Establishing the phenotype of the heterozygous, GIP-reduced mouse is important to understand the possible benefits of limited reduction of GIP secretion.

Research design and methods

Animals. Male GIP-GFP KI mice and wild-type littermates (WT) were used in all experiments. GIP-GFP KI mice were generated as described previously (15). The animals were maintained in conditions of 12 h of light cycle and 12 h of dark cycle, with free access to water and food, unless indicated otherwise. Starting from 7 weeks of age, the mice were divided into two groups: control fat diet (CFD) group, receiving food with 10% of fat and energy density of 3.8 kcal/g (Research Diets Inc. New Brunswick, NJ, USA; cat.no.D12450B), and high fat diet (HFD) group, receiving food with 60% of fat and energy density of 5.2 kcal/g (Research Diets Inc. New Brunswick, NJ, USA; cat.no.D12492). In total, 6 groups of mice (5-6 mice per group) were used throughout the study: WT on CFD, heterozygous GIP-GFP KI mice ($GIP^{gfp/+}$) on CFD, homozygous GIP-GFP KI mice ($GIP^{gfp/gfp}$) on CFD, WT on HFD, heterozygous GIP-GFP KI mice ($GIP^{gfp/+}$) on HFD and homozygous GIP-GFP KI mice ($GIP^{gfp/gfp}$) on HFD. After 8 weeks of control fat or high fat feeding, the animals were used in the experiments listed below. Maintenance of the mice and all experimental procedures were approved by Kyoto University Animal Care Committee.

Expression levels of GIP receptor (GIPR) mRNA. After standard chow feeding or at least 8 weeks of CFD and HFD, mice were sacrificed by cervical dislocation, and pancreas and white (visceral) adipose tissue were harvested. The white adipose tissue was frozen immediately in liquid nitrogen and stored at -80°C until further use; pancreas was digested using collagenase method and islets were obtained. Islet mRNA (RNeasy Mini Kit, Qiagen, Hilden, Germany) and adipose tissue mRNA (RNeasy Lipid Tissue Mini Kit, Qiagen, Hilden, Germany) were extracted

and cDNA (complementary DNA) was synthesized by reverse transcription (SuperScript II, Invitrogen, NY, USA). GIPR mRNA expression levels were quantified by semi-quantitative real-time polymerase chain reaction (RT-PCR) (Applied Biosystems, AB StepOne Plus Real Time PCR, Foster City, CA, USA) using GIPR forward and reverse primer with the following sequence: 5'-CCTCCACTGGGTCCCTACAC-3' (forward primer) and 5'-GATAAACACCCTCCACCAGTAG-3' (reverse primer). GAPDH mRNA was used as an internal control. The sequences of GAPDH forward and reverse primer are as follows: 5'-AAATGGTGAAGGTCGGTGTG-3' for the forward primer and 5'-TCGTTGATGGCAACAATCTC-3' for the reverse primer.

Measurement of GIP content and protein content. Mice at the age of 6 weeks were sacrificed by cervical dislocation, intestine samples were taken and washed in phosphate buffer saline (PBS), weight was measured and, after overnight extraction with 5 ml/g acid ethanol (at 4°C), GIP content was measured by ELISA (Millipore Corp, Bilerica, MA, USA). Protein content was measured using Bradford Protein Assay (Bio-Rad, Hercules, CA, USA). In brief, dye reagent was diluted and protein (albumin) standards were made in duplicate. Standards and intestine samples were loaded on a micro titer plate, incubated at room temperature for 5 min and absorbance was read at 595 nm. GIP content was expressed as GIP content per protein content.

Bone histomorphometry. Mice at the age of 6 weeks kept on standard chow were prepared for bone histomorphometry measurement by injecting subcutaneously 25 mg/kg of tetracycline hydrochloride (Sigma-Aldrich, St.Louis, MO, USA) 4 days before sacrifice and 10 mg/kg of calcein (Dojindo, Kumamamoto, Japan) 2 days before sacrifice. Animals were sacrificed by cervical dislocation and tibiae were removed and fixed with 70% ethanol. Further processing of tibiae samples (muscle removing, dehydration in graded concentration of ethanol, Villanueva

bone staining and embedding in methyl-metacrylate), preparation of frontal plane sections of tibiae and bone histomorphometry measurement using semiautomatic image analyzing system (System Supply, Nagano, Japan) were done by Niigata Bone Science Institute, Niigata, Japan.

Oral glucose tolerance test (OGTT) and measurement of hormones. Following 8 weeks of CFD and HFD, the mice underwent oral glucose tolerance test (OGTT). The fasting period (overnight fasting) was begun 19 h prior to the experiment. During the test, blood samples were taken by heparinized micro-capillary tubes from the orbital sinus of the mice at the following time intervals: 0 min (fasting levels), 15, 30, 60, and 120 min after glucose administration. Glucose (2 g/kg in mice on standard chow and 1 g/kg in mice on HFD) was given orally, using gavage tube. Blood glucose levels were measured by glucose oxidase method (Sanwa Kagaku Kenkyusho CO. LTD., Nagoya, Japan). After collecting the blood samples, they were kept on ice, and then centrifuged (3000 rpm/10 min/4°C) and serum was separated. The serum samples were used fresh or kept at -80°C until further processing. Insulin, total GIP, and total GLP-1 levels were measured by ELISA as follows: insulin kit (Shibayagi, Gumma, Japan), total GIP kit (Millipore Corp, Bilerica, MA, USA), and total GLP-1 kit (MSD, Meso Scale Discovery, Rockville, MD, USA).

Insulin tolerance test (ITT). The mice were fasted 4-6 h before the start of the experiment. Blood samples were drawn from the orbital sinus using heparinized micro-capillary tubes at the following time intervals: 0 min (fasting levels), 15, 30, 60, and 120 min after insulin administration. Human insulin (100 U/ml, Eli Lilly and Co, Indianapolis, IN, USA) was administered intraperitoneally in a dose of 0.5 U/kg. Blood glucose levels were measured by glucose oxidase method (Sanwa Kagaku Kenkyusho CO. LTD., Nagoya, Japan).

Measurement of body fat composition (measurement of subcutaneous and visceral fat). In young mice at the age of 7 weeks, or after 8 weeks of CFD or HFD, body fat was measured by computerized tomography (CT) scan (A La Theta LCT-100, Aloka, Tokyo, Japan). The mice were anesthetized with intraperitoneal injection of sodium pentobarbital and placed in a measurement chamber of the CT scanner in supine position. The scanned area of the body was flanked by xiphisternum and sacrum; the width of scanned slices was 2 mm. Obtained images were analyzed using A La Theta software, version 1.00 and values of body fat, both subcutaneous and visceral, were quantified in grams (g).

Indirect calorimetry and mice activity. Mice were kept 6-7 weeks on CFD or HFD and, afterwards, indirect calorimetry was performed and activity of the mice was measured (ARCO 2000 Mass spectrometer-ARCOSYSTEM Inc, Chiba, Japan). Each mouse was placed in an individual chamber with free access to water and CFD or HFD. Respiratory quotient (RQ), energy expenditure (cal/min/kg), fat oxidation (mg/min/kg), and mice activity (counts/min) were measured every 5 min during 48 h.

In vitro insulin secretion. For measurement of glucose-stimulated insulin secretion (GSIS) *in vitro*, islets from mice on CFD and HFD were isolated using collagenase digestion method. In brief, mice were sacrificed by cervical dislocation; 0.5 mg/ml collagenase dissolved in Hanks balanced salt solution (HBSS) was injected through the bile duct into the pancreas and, after its expansion, it was manually isolated and incubated in Krebs-Ringer bicarbonate buffer (KRBB; 120 mM NaCl, 4.7 mM KCl, 1.2 mM MgSO₄, 1.2 mM KH₂PO₄, 2.4 mM CaCl₂, 20 mM NaHCO₃) at 37°C during 21 min. After homogenizing the pancreas with KRBB, the islets were separated by centrifugation in ficoll gradient. Separated islets were resuspended in KRBB on a dish and handpicked under light microscope. For GSIS assessment, three batches of different

glucose concentrations were prepared: 5.5 mM glucose, 11.1 mM glucose, and 11.1 mM glucose + 100 nM GIP-human (Peptide Institute Inc., Osaka, Japan). For each sample containing 500 μ l of incubation medium (KRBB; 2M 4-(2-hydroxyethyl)-1-piperazine ethane sulfonic acid (HEPES) pH 7.4; 0.2% Bovine Serum Albumin), 10 islets were handpicked in a volume of 200 μ l of KRBB and incubated at 37°C during 30 min (following pre-incubation in same conditions). For measurement of insulin content in islets of HFD-fed mice, samples were incubated overnight with 5 ml/g acid ethanol (at 4°C). Insulin concentration and insulin content were measured using radioimmunoassay (RIA) (Aloka Accuflex γ 7000, Hitachi, Tokyo, Japan).

Measurement of β -cell area. Whole pancreas was isolated manually from mice kept on CFD and HFD for 8 weeks. All isolated organs were fixed in Bouin's solution, afterwards washed with 50% ethanol once per day during 1 week and finally, embedded in paraffin. Every fifth section of the pancreas was used for analysis. In total, three sections (slides) per pancreas (per mouse) were analyzed. The paraffin slides were deparaffinized with lemosol, rehydrated with 100% and 70% ethanol, blocked by 3% peroxidase and incubated overnight (at 4°C) in a humidified chamber with polyclonal rabbit anti-insulin antibody (Santa Cruz Biotechnology, Santa Cruz, USA) and conjugated with fluorescent secondary antibody the next day. After immunostaining, all slides were analyzed by immunofluorescent microscope (Keyence Corp., Osaka, Japan) using BZ Analyzer software. The area of the whole pancreas and the area of insulin-immunopositive cells were measured at the same time. The β -cell area was expressed as β -cell area/total pancreas area in all analyzed slides.

Statistics. All results are expressed as mean \pm SE. Statistical analyses were performed using ANOVA with Tukey's test and P values <0.05 were considered statistically significant.

Results

1. GIP reduction in GIP-GFP KI mice

The main genetic trait of GIP-GFP KI mice is alteration (truncation) of the prepro-GIP gene coupled with insertion of GFP coding sequence (15). In mice kept on standard chow, assessment of GIP mRNA levels in the small intestine showed reduced levels in heterozygous GIP-GFP KI mice ($GIP^{gfp/+}$) ($p < 0.05$), while in homozygous mice ($GIP^{gfp/gfp}$), GIP mRNA could not be detected ($p < 0.05$, $p < 0.01$) (Fig.1A). Small-intestinal GIP content was reduced in $GIP^{gfp/+}$ ($p < 0.05$) and was undetectable in $GIP^{gfp/gfp}$ ($p < 0.01$) when compared to wild-type mice (WT). Total GIP levels during OGTT (Fig.1B) as well as GIP secretion (as shown by area under the curve of GIP (AUC-GIP)) (Fig.1C) were reduced by ~50% in $GIP^{gfp/+}$ ($p < 0.01$) and were below the lower limit of detection in $GIP^{gfp/gfp}$ ($p < 0.001$) in comparison to control (WT) (the lower detection limit of ELISA total GIP levels kit was 8.2 pg/ml).

2. Body weight progression, glucose tolerance, and β -cell profile following GIP reduction in standard chow-fed mice

Starting from 4 weeks of age, the body weight of weaning mice fed standard chow (containing 10% of fat) was recorded and it showed no changes among WT, $GIP^{gfp/+}$, and $GIP^{gfp/gfp}$ (Fig. 2A). Measurement of body fat composition (body fat) in the 7th week of age (just before placing the mice on HFD) revealed similar amount of body fat in all mice (Fig.2B). During OGTT, blood glucose levels were higher in $GIP^{gfp/+}$ than those in WT at 30 min ($p < 0.05$), whereas in $GIP^{gfp/gfp}$ glucose elevation persisted at 30 and 60 min ($p < 0.05$) (Fig.2C). Meanwhile, insulin levels in both $GIP^{gfp/+}$ and $GIP^{gfp/gfp}$ remained lower in comparison to WT, especially at 15 and 30 min after glucose load ($p < 0.05$) (Fig.2D). *In vitro* measurement of insulin secretion (Fig.2E) showed a similar pattern of secretion in all types of mice at 5.5 mM glucose, as well as

at 11.1 mM glucose. When challenged with 100 nM of human GIP peptide together with 11.1 mM glucose, the islets of GIP-GFP KI mice, both $GIP^{gfp/+}$ and $GIP^{gfp/gfp}$, exhibited a similar insulin response to that of WT. GIP receptor mRNA levels in β -cells remained unchanged in GIP-GFP KI mice when compared to control (Fig.2F). mRNA expression of preproglucagon, peptide YY, cholecystokinin, somatostatin, and secretin in the small intestine showed no differences in GIP-GFP KI mice in comparison to WT (data not shown). Plasma GLP-1 levels during OGTT did not differ among the three types of mice (WT = 15.54 ± 6.8 pg/ml, $GIP^{gfp/+}$ = 11.83 ± 4.97 pg/ml, $GIP^{gfp/gfp}$ = 18.54 ± 3.96 pg/ml at 15 min after OGTT).

Body weight follow-up of mice on CFD in a period of 8 weeks (starting at the age of 7 weeks) showed that the body weight progression did not differ among all three groups of mice (Supplementary figure 1A). The overall glucose response to 0.5 U/kg of human insulin (ITT data) was similar in WT, $GIP^{gfp/+}$, and $GIP^{gfp/gfp}$ at almost all time points of the experiment (at 60 min of ITT $GIP^{gfp/gfp}$ mice had lower blood glucose when compared to WT) (Supplementary figure 1B).

3. Bone formation in conditions of standard chow feeding

Following GIP reduction, the bone volume in $GIP^{gfp/+}$ was similar to that in WT, whereas $GIP^{gfp/gfp}$ had reduced bone volume ($p < 0.05$) (Fig.3A). Furthermore, the number of trabeculae in $GIP^{gfp/+}$ showed no changes when compared to WT, while $GIP^{gfp/gfp}$ exhibited a decrease ($p < 0.05$) (Fig.3C), as demonstrated by the images of proximal tibial sections (Fig.3B). Although osteoblast surface was decreased in $GIP^{gfp/+}$ in comparison to WT ($p < 0.05$) (Fig.3D), the bone formation rate (Fig.3F) remained unchanged in these mice. Osteoclast surface was increased in $GIP^{gfp/gfp}$ ($p < 0.05$) when compared to WT, while in $GIP^{gfp/+}$ it remained similar to WT (Fig.3E).

4. Induction of metabolic stress by HFD

Figures 4 and 5 describe the phenotype changes induced by HFD feeding for 8 weeks (56 days). Starting from the second week of HFD, WT mice steadily increased their body weight ($p < 0.001$) in comparison to the lean control (Fig.4A), while within the HFD group, $GIP^{gfp/+}$ showed lesser body weight gain ($p < 0.01$ at 2nd week; $p < 0.001$ at 8th week) than WT; $GIP^{gfp/gfp}$ exhibited lowest body weight gain ($p < 0.001$ at 2nd week; $p < 0.001$ at 8th week vs. WT HFD). Ad libitum glucose levels were measured at the same time, once per week, and the overall glucose levels in all mice remained similar (Fig.4B). Food and water intake were similar in all groups of mice (data not shown).

During OGTT, total GIP levels and GIP secretion were increased 2-fold in WT on HFD ($p < 0.001$) as compared to the lean control; in HFD-fed mice, $GIP^{gfp/+}$ exhibited decreased levels ($p < 0.05$), while $GIP^{gfp/gfp}$ showed an absence of GIP ($p < 0.001$) (Fig.4C and 4D). Fasting glucose levels in WT on HFD were higher ($p < 0.01$) when compared to their lean littermates; on HFD background, glucose levels remained similar in all mice (Fig.4E). The overall insulin response (Fig.4F) in WT on HFD was more intense than that of the control mice, and, within the HFD group, the insulin levels of $GIP^{gfp/+}$ remained lower in comparison to WT ($p < 0.05$), while $GIP^{gfp/gfp}$ showed the lowest insulin levels ($p < 0.01$, $p < 0.001$). Insulin secretion *in vitro* (Fig.4G) was similar among all mice on CFD and HFD in the presence of 5.5 mM glucose. In response to 11.1 mM glucose, WT on HFD had higher insulin secretion compared to WT on CFD, whereas in the HFD group similar levels were found in WT and $GIP^{gfp/+}$, coupled with lower insulin in $GIP^{gfp/gfp}$ ($p < 0.05$ vs. WT HFD, $p < 0.01$ vs. $GIP^{gfp/+}$). When 100 nM of human GIP peptide were added to 11.1 mM glucose, insulin secretion remained lower in $GIP^{gfp/gfp}$ on HFD ($p < 0.01$). Measurement of β -cell area, as expressed by the ratio of β -cell area/total pancreas area, showed tendency to an increase observed in HFD-fed mice, relative to the lean mice, although the

difference was not statistically significant. However, within HFD group, β -cell area remained similar in WT and $GIP^{gfp/+}$, while $GIP^{gfp/gfp}$ exhibited decreased β -cell area ($p < 0.05$) (Fig.4H). The expression levels of GIP receptor (GIPR) mRNA in the islets were similar in WT mice on CFD and HFD, as well as in $GIP^{gfp/+}$ on HFD, while in $GIP^{gfp/gfp}$ they were reduced ($p < 0.01$ vs. $GIP^{gfp/+}$) (Fig.4I).

5. Adipose tissue response to HFD feeding and consequential energy expenditure changes

CT scan measurement (Fig.5A) of visceral, subcutaneous, and total body fat demonstrated a large increase in fat accumulation in WT on HFD ($p < 0.01$) when compared to the lean mice. On a HFD background, WT accumulated more body fat than their $GIP^{gfp/+}$ littermates ($p < 0.05$), while the fat depots in $GIP^{gfp/gfp}$ were greatly reduced ($p < 0.01$), showing levels similar to the lean control. The CT scan images of abdominal sections of mice on CFD and HFD visualize the difference in fat accumulation among all groups. Assessment of insulin resistance by insulin tolerance test (ITT) (Fig.5B) showed a rise of glucose levels in HFD-fed WT as compared to the lean mice, while within the HFD group, a better response to insulin was observed in both $GIP^{gfp/+}$ and $GIP^{gfp/gfp}$, glucose levels remaining lower ($p < 0.05$; $p < 0.01$) in comparison to WT. In relation to these data, a tendency towards increased fat oxidation (Fig.5C) in all mice on HFD was observed ($p < 0.05$), with a larger increase in $GIP^{gfp/+}$ ($p < 0.05$), especially in the dark phase and, even higher, in $GIP^{gfp/gfp}$ ($p < 0.05$). In addition, energy expenditure measurement on HFD background (Fig.5D) showed an increase in $GIP^{gfp/+}$ ($p < 0.05$) (again, more prominent in the dark phase) and in $GIP^{gfp/gfp}$ ($p < 0.05$) when compared to WT. Concomitantly, mice activity was measured (Fig.5E), and no statistically significant changes were found in the HFD group. Expression levels of GIPR mRNA in white (visceral) adipose tissue (Fig.5F) remained

unchanged in all animals on CFD and HFD, except for GIP^{gfp/gfp}, in which the levels were elevated ($p < 0.05$).

Discussion

Studies in single and double incretin receptor knock-out mice (DIRKO) (16) have shown that although secretion of GIP and GLP-1 is triggered by different factors, they have an additive stimulating effect on β -cells with regard to insulin secretion, with GIP accounting for the larger portion of the total incretin effect in male mice. Furthermore, human data demonstrated that after oral glucose load of 75 g and after mixed meal load (17, 18), secretion of GIP is more pronounced than GLP-1 secretion, suggesting that GIP may play a more potent role in regulation of postprandial insulin secretion in non-diabetic conditions. We have generated GIP-GFP KI mice characterized by truncation of the prepro-GIP gene and insertion of GFP coding sequence that leads to reduced GIP production in heterozygous state and absence of GIP production in homozygous state. GIP^{gfp/gfp} exhibit a phenotype similar to GIPRKO mice regarding glucose tolerance, bone formation, and adipose tissue expansion (Table 1). However, GIP^{gfp/+} represent a novel mouse model in which GIP, despite its secretion being reduced by half, maintains glucose levels similar to controls (Fig. 4B and Fig.4E) and lessens insulin resistance in high fat diet-induced obesity (Fig.4F and Fig.5B).

When fed standard chow, GIP-lacking mice (GIP^{gfp/gfp}), similarly to GIPRKO mice, had higher glucose excursions accompanied with insufficient production of insulin during OGTT (Table 1). In spite of having reduced, but still present GIP secretion, GIP-reduced mice (GIP^{gfp/+}) also showed mild glucose intolerance and lower insulin secretion, confirming the potent insulinotropic effect of GIP (Fig.2C, Fig. 2D, and Table 1). Furthermore, insulin secretion tests *in vitro* demonstrated a similar pattern of secretion in all groups of mice. Measurement of mRNA

expression levels of GIPR in the islets showed no changes among all groups of mice, indicating the presence of functional GIP receptors.

Similarly to GIP-lacking and GIP-reduced mice, rat GIP promoter-diphtheria toxin A chain transgenic mice (GIP/DT) exhibit glucose intolerance, in their case very profound, with complete abolition of the incretin effect, and show similarities in phenotype under high fat diet conditions (19). In this mouse model (GIP/DT), forced expression of attenuated diphtheria toxin was established under rat GIP promoter, leading to isolated ablation of GIP-producing cells and, subsequently, absence of GIP mRNA transcripts and absence of circulating GIP levels. However, there are reports confirming the existence of double incretin-positive cells (K/L cells) in the intestine (20) and an existence of populations of K-cells that co-express not only GIP but also glucagon, somatostatin, secretin and, to a smaller extent, some other hormones as well (21, 22). Therefore, ablation of K-cells might affect the number and/or distribution of these cell populations and could influence the accurate assessment of secretion of various intestinal hormones. In the case of GIP-GFP KI mice, the truncation of the prepro-GIP gene and expression of GIP-GFP fusion protein were driven by native GIP promoter, enabling selective changes in K-cells that affect only GIP secretion and, even more importantly, control of the levels of GIP production. The expression levels of mRNA of the intestinal hormones preproglucagon, peptide YY, cholecystokinin, somatostatin and secretin were not changed, confirming that GIP reduction did not interfere with their gene expression.

There are reports demonstrating that GIP induces GLP-1 secretion (23, 24). Previously conducted studies of disrupted or blocked GIPR signaling (7, 16, and 19) did not show information regarding the secretion of GLP-1. In our study, plasma GLP-1 levels remained unchanged in GIP-GFP KI mice, as reported earlier in a model of GIPR antagonism (14),

indicating that reduction of GIP secretion does not affect GLP-1 secretion. Overall, GIP-reduced mice kept on standard chow after birth did not exhibit visible abnormalities regarding mating potential, pregnancy, offspring viability, growth, organ composition, and feeding behavior (data not shown). Measurement of their body weight from the beginning of the weaning period (Fig.2A) until just before the shift to high fat diet (HFD), as well as longer term measurement (Supplementary figure 1A), showed that they are not different from their wild type littermates when fed standard diet. Body fat measured before the start of the HFD was similar between WT and GIP-GFP KI mice. Insulin tolerance test showed that their insulin sensitivity remained similar to the WT mice (Supplementary figure 1B).

In addition to its insulinotropic role, GIP is involved in modulation of bone formation. There are GIP-specific receptors located on osteoblasts (25) and osteoclasts (26). GIP operates as an anabolic hormone in the bone, where it stimulates incorporation of meal-derived Ca^{2+} into bone and bone building (13) and reduces bone absorption by inhibiting osteoclastic activity. Studies in GIPRKO mice have shown that the absence of GIPR signaling leads to significant osteoporosis due to lower osteoblast and higher osteoclast action (13). Similarly to GIPRKO mice, GIP-lacking mice also showed signs of osteoporosis, manifested by reduced bone volume, reduced number of trabeculae and increased osteoclast surface. On the other hand, GIP-reduced mice maintained normal bone volume and bone trabeculae, and, despite the exhibited reduction of osteoblast surface, no increased osteoclast activity was observed. More importantly, the bone formation rate remained normal, indicating that reduction of GIP by ~50% does not significantly impair the beneficial role of GIP in bone formation. Considering the glucose intolerance of these mice, it appears that reduction of GIP secretion more profoundly affects the insulin-potentiating

role of GIP, indicating differing regulatory mechanisms of GIP action in β -cells and in bone (Table 1).

To better understand the extent of the phenotypic consequences following GIP reduction, we induced chronic metabolic stress by feeding the mice with high fat diet (HFD). Previous reports indicate a strong connection between GIP secretion and obesity in high fat diet-feeding conditions (27). High caloric intake causes hypersecretion of GIP (12, 28, and 29) due to hyperexpression of the GIP gene (15) and a subsequent rise in insulin secretion (30), leading to increased fat deposition in the adipose tissue and expansion of fat depots (31, 32). GIP increases the adipose tissue volume directly (33, 34) by binding to its receptors located on the adipocytes and indirectly by potentiating β -cell secretion of insulin, which is known to be involved in adipocyte fat deposition (35). In our study, HFD-feeding for at least 8 weeks resulted in absence of circulating GIP levels in GIP-lacking mice (consistent with data from standard chow-fed mice), while in GIP-reduced mice, reduction of GIP was similar to the levels observed in lean WT and was lower when compared to WT on HFD. The most obvious consequence of HFD was a change in body weight and fat mass in WT and GIP-GFP KI mice (Fig.4A, Fig.5A, and Table 1). While WT showed overt obesity, GIP-lacking mice retained their body weight and fat mass at levels similar to those of their lean littermates, as previously reported in GIPRKO mice, in mice with K-cell ablation (19), and in mice with chemical inhibition of GIPR signaling (14). GIP-reduced mice also maintained lower body weight throughout the experiment period of 56 days, indicating that while the lack of body weight gain and fat mass was not as evident as it was in GIP-lacking mice, the reduced obesity was nevertheless important. Moreover, the glucose response to insulin during ITT showed lower levels in both GIP-reduced and GIP-lacking mice fed HFD, indicating that not only complete, but also partial reduction of GIP alleviates insulin

resistance while reducing obesity. Thus, a reduction of GIP secretion as shown in GIP-reduced mice mitigates both direct and indirect actions of GIP on adipose tissue and leads to reduced diet-induced obesity.

Glucose levels measured ad libitum throughout most of the experiment period were similar in WT mice and GIP-GFP KI mice, and glucose excursions during OGTT remained similar as well in all mice under HFD condition. However, all HFD-fed mice had higher OGTT glucose levels when compared to the lean controls, suggesting that when metabolic stress was introduced, glucoregulation was similarly achieved in conditions of normal and reduced GIP production. At the same time, the circulating insulin levels were lower in GIP-lacking and GIP-reduced mice than those of WT on HFD, accompanied by decreased insulin resistance (Fig.5B and Table 1). This data is in line with a previous study examining the role of insulin in obesity and showing that on an obese background, reduction of insulin not necessarily causes severe disturbance in blood glucose levels (36). The origins of the reduced insulin secretion are associated not only with reduced GIP signaling in β -cells, but with changes in their area as well. While GIP-reduced mice had similar β -cell area to their WT counterparts on HFD, GIP-lacking mice had clearly less β -cells. Furthermore, *in vitro* islet studies found that the responsiveness of β -cells to glucose in GIP-reduced mice was similar to that in WT on HFD and was higher than that of the control mice. On the other hand, GIP-lacking mice had reduced insulin response to glucose, suggesting that reduction of GIP secretion might affect the ability of β -cells to respond adequately to GIP, but not as profoundly as in cases of complete absence of GIP secretion or GIPR signaling. Measurement of GIPR mRNA levels in the islets revealed similar values in WT and GIP-reduced mice, while GIP-lacking mice exhibited decreased expression of GIPR mRNA. GIPR mRNA expression levels in the adipose tissue did not show changes in WT and GIP-reduced mice but,

interestingly, they were increased in GIP-lacking mice, which is inconsistent with the islet data. Although previous studies have extensively addressed disruption of GIPR signaling, our GIP-lacking mice show for the first time a condition of complete lack of GIP secretion from intact K-cells and might be useful in further studies.

We have investigated the mechanism of regulation of glucose homeostasis and reduced obesity in GIP-GFP KI on HFD. Previously, we reported an increase in fat oxidation and energy expenditure in GIPRKO mice fed HFD for a short period (37) and in GIPRKO mice with diminished insulin signaling (insulin receptor substrate 1 (IRS1) KO/GIPRKO mice) (38), indicating that increased fat oxidation accounts for the reduction of obesity in the absence of GIPR signaling. The present study has demonstrated increased fat oxidation in GIP-reduced, and, even more intensely, in GIP-lacking mice. This phenomenon might occur due to increased adiponectin levels via peroxisome proliferator-activated receptor alpha (PPAR α) levels in the adipose tissue (37) or due to increased activity of the enzymes involved in beta oxidation in liver, such as cluster of differentiation 36 (CD36) and mitochondrial uncoupling protein 2 (UCP2) (38). GIP-lacking and GIP-reduced mice also exhibited higher energy expenditure on HFD. There are reports showing that increased energy expenditure is coupled with increased locomotor activity; disruption of GIPR signaling increases mice activity not only in high fat diet conditions, as in mice treated with GIPR antagonist (14) and GIPRKO mice (12), but leads to increased spontaneous activity even during standard diet feeding, as described in DIRKO mice (29) and in adult or aged GIPRKO mice (39, 40). Consistent with these data, GIP-lacking and GIP-reduced mice also exhibited a tendency toward increased mice activity, especially in the dark phase, although without statistically significant difference.

In conclusion, our data suggest that reduction of GIP secretion *in vivo* confirms the potent role of GIP in insulin secretion and leads to reduced obesity and reduced insulin resistance in high fat diet conditions without severely impairing glucose homeostasis and without disrupting the role of GIP in bone formation. These findings are potentially promising of a new therapeutic approach to obesity and type 2 diabetes mellitus.

Acknowledgements

The authors thank Mr. Shoichi Asano and Dr. Xibao Liu from the Department of Diabetes, Endocrinology and Nutrition, Graduate School of Medicine, Kyoto University, for their technical support regarding the study. This study was supported by Scientific Research Grants from the Ministry of Education, Culture, Sports, Science, and Technology, Japan, and from the Ministry of Health, Labor, and Welfare, Japan.

D.N., N.H., K.Su., S.Y., A.H., E.J., K.I., K.Sh., and T.H. have no conflict of interest to disclose.

N.I. served as a medical advisor for Takeda, Taisho Pharmaceutical, GlaxoSmithKline, Mitsubishi Tanabe Pharma, he lectured for MSD, Sanofi, Novartis Pharma, Dainippon Sumitomo Pharma, Kyowa Kirin, and Mitsubishi Tanabe Pharma, and received payment for his services. N.I. also received a clinical commissioned/joint research grant from MSD, Eli Lilly Japan, Shiratori Pharmaceutical, Roche Diagnostics, and the Japan Diabetes Foundation, and also received a scholarship grant from MSD, JT, Nippon Boehringer Ingelheim, Takeda, Dainippon Sumitomo Pharma, Astellas Pharma, Daiichi-Sankyo, and Mitsubishi Tanabe Pharma.

D.N. researched the data, contributed to discussion, wrote, reviewed and edited the manuscript.

N.H. contributed to discussion, reviewed and edited the manuscript. K.Su., S.Y., A.H., E.J., K.I., K.Sh., and T.H. contributed to discussion. N.I contributed to discussion, reviewed and edited the manuscript.

N.I. is the guarantor of this work and, as such, had full access to all the data in the study and takes responsibility for the integrity of the data and the accuracy of the data analysis.

Parts of the study were presented in an abstract form at the 47th Annual Meeting of the European Association for the study of Diabetes in Lisbon, Portugal, 12-16 September 2011, at the 48th Annual Meeting of the European Association for the study of Diabetes in Berlin, Germany, 1-5 October 2012, and at the 73rd Scientific Sessions of the American Diabetes Association in Chicago, Illinois, 21-25 June 2013.

References:

1. Krarup T, Holst JJ, Lindorf Larsen K. Responses and molecular heterogeneity of IR-GIP after intraduodenal glucose and fat. *Am J Physiol.* 1985; 249 (2 Pt 1): E195-E200.
2. Flatt PR. Dorothy Hodgkin Lecture 2008 Gastric inhibitory polypeptide (GIP) revisited: a new therapeutic target for obesity–diabetes? *Diabetic Med.* 2008; 25 (7): 759-764.
3. Baggio LL, Drucker DJ. Biology of incretins: GLP-1 and GIP. *Gastroenterology.* 2007; 132 (6): 2131-2157.
4. Pederson RA, Brown JC. Inhibition of histamine-, pentagastrin-, and insulin-stimulated canine gastric secretion by pure "gastric inhibitory polypeptide". *Gastroenterology.* 1972; 62 (3): 393-400.
5. Dupre J, Ross SA, Watson D, Brown JC. Stimulation of insulin secretion by gastric inhibitory polypeptide in man. *J Clin Endocrinol Metab.* 1973; 37 (5): 826-828.
6. Yamada Y, Miyawaki K, Tsukiyama K, Harada N, Yamada C, Seino Y. Pancreatic and extrapancreatic effects of gastric inhibitory polypeptide. *Diabetes.* 2006; 55, Supplement 2, S86-S91.
7. Miyawaki K, Yamada Y, Yano H et al. Glucose intolerance caused by a defect in the entero-insular axis: A study in gastric inhibitory polypeptide receptor knockout mice. *P Natl Acad Sci USA.* 1999; 96 (26): 14843-14847.
8. Herbach N, Bergmayr M, Göke B, Wolf E, Wanke R. Postnatal development of numbers and mean sizes of pancreatic islets and beta-cells in healthy mice and GIPR^{dn} transgenic diabetic mice. *PLoS ONE.* 2011; 6 (7): e22814.
9. Renner S, Fehlings C, Herbach N et al. Glucose intolerance and reduced proliferation of pancreatic β -cells in transgenic pigs with impaired glucose-dependent insulinotropic peptide function. *Diabetes.* 2010; 59 (5): 1228-1238.
10. Kim SJ, Winter K, Nian C, Tsuneoka M, Koda Y, McIntosh CH. Glucose-dependent insulinotropic polypeptide (GIP) stimulation of pancreatic β -cell survival is dependent upon phosphatidylinositol 4-kinase (PI3K)/protein kinase B (PKB) signaling, inactivation of the forkhead transcription factor Foxo1, and downregulation of bax expression. *J Biol Chem.* 2005; 280 (23): 22297-22307.

11. Widenmaier SB, Kim SJ, Yang GK et al. A GIP receptor agonist exhibits β -cell anti-apoptotic actions in rat models of diabetes resulting in improved β -cell function and glycemic control. *PLoS One*. 2010; 5 (3): e9590.
12. Miyawaki K, Yamada Y, Ban N et al. Inhibition of gastric inhibitory polypeptide signaling prevents obesity. *Nat Med*. 2002; 8 (7): 738-742.
13. Tsukiyama K, Yamada Y, Yamada C et al. Gastric inhibitory polypeptide as an endogenous factor promoting new bone formation after food ingestion. *Mol Endocrinol*. 2006; 20 (7): 1644-1651.
14. McClean PL, Irwin N, Cassidy RS, Holst JJ, Gault VA, Flatt PR. GIP receptor antagonism reverses obesity, insulin resistance, and associated metabolic disturbances induced in mice by prolonged consumption of high-fat diet. *Am J Physiol Endocrinol Metab*. 2007; 293 (6): E1746-E1755.
15. Suzuki K, Harada N, Yamane S et al. Transcriptional regulatory factor X6 (Rfx6) increases gastric inhibitory polypeptide (GIP) expression in enteroendocrine K-cells and is involved in GIP hypersecretion in high fat diet-induced obesity. *J Biol Chem*. 2013; 288 (3): 1929-1938.
16. Preitner F, Ibberson M, Franklin I et al. Gluco-incretins control insulin secretion at multiple levels as revealed in mice lacking GLP-1 and GIP receptors. *J Clin Invest*. 2004; 113 (4): 635-645.
17. Yamane S, Harada N, Hamasaki A et al. Effects of glucose and meal ingestion on incretin secretion in Japanese subjects with normal glucose tolerance. *J Diabetes Invest*. 2012; 3 (1) 80-85.
18. Vollmer K, Holst JJ, Baller B et al. Predictors of incretin concentrations in subjects with normal, impaired, and diabetic glucose tolerance. *Diabetes*. 2008; 57 (3): 678-687.
19. Althage MC, Ford EL, Wang S, Tso P, Polonsky KS, Wice BM. Targeted ablation of glucose-dependent insulinotropic polypeptide-producing cells in transgenic mice reduces obesity and insulin resistance induced by high fat diet. *J Biol Chem*. 2008; 283 (26): 18365-18376.
20. Fujita Y, Chui JWY, King DS et al. Pax6 and Pdx1 are required for production of glucose-dependent insulinotropic polypeptide in proglucagon-expressing L cells. *Am J Physiol Endocrinol Metab*. 2008; 295 (3): E648-E657.
21. Parker HE, Habib AM, Rogers GJ, Gribble F, Reimann F. Nutrient-dependent secretion of glucose-dependent insulinotropic polypeptide from primary murine K cells. *Diabetologia*. 2009; 52 (2): 289-298.
22. Habib AM, Richards P, Cairns LS et al. Overlap of endocrine hormone expression in the mouse intestine revealed by transcriptional profiling and flow cytometry. *Endocrinology*. 2012; 153 (7): 3054-3065.
23. Brubaker PL. Regulation of intestinal proglucagon-derived peptide secretion by intestinal regulatory peptides. *Endocrinology*. 1991; 128 (6): 3175-3182.
24. Roberge JN, Brubaker PL. Regulation of proglucagon-derived peptide secretion by glucose-dependent insulinotropic peptide in a novel enteroendocrine loop. *Endocrinology*. 1992; 133 (1): 233-240.
25. Pacheco-Pantoja EL, Ranganath LR, Gallager JA, Wilson PJM, Fraser WD. Receptors and effects of gut hormones in three osteoblastic cell lines. *BMC Physiol*. 2011; 11:12 1-14.

26. Zhong Q, Itokawa T, Sridhar S et al. Effects of glucose-dependent insulinotropic peptide on osteoclast function. *Am J Physiol Endocrinol Metab.* 2007; 292 (2): E543-E548.
27. Kieffer TJ. GIP or not GIP? That is the question. *Trends Pharmacol Sci* 2003; 24(3):110-2.
28. Creutzfeldt W, Ebert R, Willms B et al. Gastric inhibitory polypeptide (GIP) and insulin in obesity: increased response to stimulation and defective feedback control of serum levels. *Diabetologia.* 1978; 14 (1): 15-24.
29. Hansotia T, Maida A, Flock G et al. Extrapancreatic incretin receptors modulate glucose homeostasis, body weight, and energy expenditure. *J Clin Invest.* 2007; 117 (1): 143-152.
30. Harada N, Yamada Y, Tsukiyama K et al. A novel GIP receptor splice variant influences GIP sensitivity of pancreatic beta-cells in obese mice. *Am J Physiol Endocrinol Metab.* 2008; 294 (1): E61-E68.
31. Harada N, Hamasaki A, Yamane S et al. Plasma gastric inhibitory polypeptide and glucagon-like peptide-1 levels after glucose loading are associated with different factors in Japanese subjects. *J Diabetes Invest.* 2011; 2 (3): 193-199.
32. Seino Y, Yabe D. Glucose-dependent insulinotropic polypeptide and glucagon-like peptide-1: Incretin actions beyond the pancreas. *J Diabetes Invest.* 2013; 4 (2): 108-130.
33. Knapper JME, Puddicombe SM, Morgan LM, Fletcher JM. Investigations into the actions of glucose-dependent insulinotropic polypeptide and glucagon-like peptide-1 (7-36) on lipoprotein lipase activity in explants of rat adipose tissue. *J Nutr.* 1995; 125: 183-188.
34. Song DH, Getty-Kaushik L, Tseng E, Simon J, Corkey BE, Wolfe MM. Glucose-dependent insulinotropic polypeptide enhances adipocytes development and glucose uptake in part through Akt activation. *Gastroenterology.* 2007; 133 (6): 1796-1805.
35. Parkin SM, Walker K, Ashby P, Robinson DS. Effects of glucose and insulin on the activation of lipoprotein lipase and on protein synthesis in rat adipose tissue. *Biochem J.* 1980; 188 (1): 193-199.
36. Mehran AE, Templeman NM, Brigidi GS et al. Hyperinsulinemia drives diet-induced obesity independently of brain insulin production. *Cell Metab* 2012; 16(6):723-37.
37. Naitoh R, Miyawaki K, Harada N et al. Inhibition of GIP signaling modulates adiponectin levels under high-fat diet in mice. *Biochem Biophys Res Commun.* 2008; 376 (1): 21-25.
38. Zhou H, Yamada Y, Tsukiyama K et al. Gastric inhibitory polypeptide modulates adiposity and fat oxidation under diminished insulin action. *Biochem Biophys Res Commun.* 2005; 335 (3): 937-942.
39. Faivre E, Gault VA, Thorens B, Hölscher C. Glucose-dependent insulinotropic polypeptide receptor knockout mice are impaired in learning, synaptic plasticity and neurogenesis. *J Neurophysiol.* 2011; 105 (4): 1574-1580.
40. Yamada C, Yamada Y, Tsukiyama K et al. Genetic inactivation of GIP signaling reverses aging-associated insulin resistance through body composition changes. *Biochem Biophys Res Commun.* 2007; 364 (1): 175-180.

Figure legends:

Figure 1. GIP reduction in GIP-GFP KI mice. Following measurements were conducted in small intestine of WT, GIP^{gfp/+} and GIP^{gfp/gfp} mice: assessment of GIP mRNA levels (expressed as GIPR mRNA/GAPDH mRNA) and GIP content (expressed as GIP/protein content) (A). Total GIP levels (B) and GIP secretion (AUC-GIP) (C) were measured during OGTT (glucose 2g/kg of body weight). n=5-6 per group. WT mice are represented by white bars and white circles, GIP^{gfp/+} mice by black bars and black squares, and GIP^{gfp/gfp} mice by gray bars and gray triangles. *p<0.05, **p<0.01, ***p<0.001.

Figure 2. Body weight, glucose tolerance and β -cell profile following GIP reduction in standard chow-fed mice

Body weight (A) of weaning mice (4 weeks-old) was measured starting from the beginning of the weaning period until the age of 8 weeks (body weight in the 7th week of age was not measured due to CT scan measurement and post-anesthesia recovery period). Body fat (B) was measured by CT scan in the 7th week of age. Glucose (C) and insulin levels (D) were measured during OGTT (glucose load of 2g/kg of body weight). *In vitro* insulin secretion from isolated islets (E) was measured in conditions of 5.5 mM glucose, 11.1 mM glucose, and 11.1 mM glucose + 100 nM human GIP peptide. GIP receptor mRNA levels in islets (F) were expressed as GIPR mRNA/GAPDH mRNA. n= 5-6 mice or samples per group; 10 islets per sample. WT mice are represented by white circles and white bars, GIP^{gfp/+} mice by black squares and black bars, and GIP^{gfp/gfp} mice by gray triangles and gray bars. *p<0.05, **p<0.01 vs. WT; #p<0.05 vs. GIP^{gfp/+} mice.

Figure 3. Bone formation in conditions of standard chow feeding. Following parameters were measured by bone histomorphometry: bone volume (expressed as bone volume %) (A),

trabeculae number (expressed as number/mm) (C), osteoblast surface (%) (D), osteoclast surface (%) (E), and bone formation rate (%/year) (F). Images display trabeculae of proximal tibial sections (B) taken from 6 weeks-old mice. $n=5-6$ per group. WT mice are represented by white bars, $GIP^{gfp/+}$ mice by black bars, and $GIP^{gfp/gfp}$ mice by gray bars. $*p<0.05$ vs. WT. Absence of asterisk above the horizontal brackets in Fig. 3A, 3C, 3D and 3E indicates no statistical significance.

Figure 4. Induction of metabolic stress by HFD. Body weight (A) and ad libitum glucose levels (B) in WT CFD, WT HFD, $GIP^{gfp/+}$ HFD and $GIP^{gfp/gfp}$ HFD mice were measured once per week during 8 weeks (56 days) of CFD (10% of fat) or HFD (60% of fat). Total GIP levels (C), GIP secretion (GIP-AUC) (D), glucose levels (E), and insulin levels (F) were measured during OGTT (glucose load of 1g/kg of body weight) conducted after 8 weeks (56 days) of CFD or HFD. *In vitro* insulin secretion from isolated islets (G) was measured in conditions of 5.5 mM glucose, 11.1 mM glucose and 11.1 mM glucose + 100 nM human GIP peptide. Results were expressed as insulin secretion (% insulin content). β -cell area (H) was measured by immunohistochemistry of pancreas sections and subsequent analysis using BZ Analyzer software. Results are expressed as β -cell area/total pancreas area. GIP receptor mRNA levels in islets (I) were expressed as GIPR mRNA/GAPDH mRNA. $n= 5-6$ mice or samples per group; 10 islets per sample. WT CFD mice are represented by white circles with square dot dash and white bars with square dot border, WT HFD mice by white circles with solid dash and white bars with solid border, $GIP^{gfp/+}$ mice by black squares and black bars, and $GIP^{gfp/gfp}$ mice by gray triangles and gray bars. P values are expressed as follows: Fig.4A, 4C, 4D, 4E, 4F: $*p<0.05$, $**p<0.01$, $***p<0.001$ vs. WT HFD. Fig.4B: $*p<0.05$ WT CFD vs. WT HFD and $\#p<0.05$ $GIP^{gfp/+}$ HFD vs.

WT HFD. Fig.4G, 4H and 4I: * $p < 0.05$, ** $p < 0.01$, *** $p < 0.001$. Absence of asterisk above the horizontal brackets in Fig. 4G, 4H and 4I indicates no statistical significance.

Figure 5. Adipose tissue response to HFD feeding and consequential energy expenditure changes. Visceral, subcutaneous and total fat (expressed in g) in WT CFD, WT HFD, $GIP^{gfp/+}$ HFD and $GIP^{gfp/gfp}$ HFD mice (A) were measured, and CT images of transversal abdominal sections were taken after 8 weeks of CFD (10% of fat) or HFD (60% of fat). ITT (insulin 0.5 U/kg of body weight) was conducted after 8 weeks of CFD or HFD (B). Fat oxidation (mg/min/kg) (C), energy expenditure (cal/min/kg) (D) and mice activity (counts/min) (E) were measured after 6-7 weeks of CFD or HFD. GIP receptor mRNA levels in white (visceral) adipose tissue (F) were expressed as $GIPR$ mRNA/ $GAPDH$ mRNA. $n = 5-6$ mice or samples per group. WT CFD mice are represented by white bars with square dot border and white circles with square dot dash, WT HFD mice by white bars with solid border and white circles with solid dash, $GIP^{gfp/+}$ HFD mice by black bars and black squares, and $GIP^{gfp/gfp}$ HFD mice by gray bars and gray triangles. P values are expressed as follows: Fig.5B * $p < 0.05$, ** $p < 0.01$, *** $p < 0.001$ vs. WT HFD; Fig. 5A, 5C, 5D, and 5F * $p < 0.05$, ** $p < 0.01$. Absence of asterisk above the horizontal brackets in Fig. 5A, 5C, 5D, and 5F indicates no statistical significance.

Supplementary figure 1. Body weight progression and insulin sensitivity in standard chow-fed mice. Body weight (A) of WT, $GIP^{gfp/+}$, and $GIP^{gfp/gfp}$ mice on CFD was measured once per week during 8 weeks (56 days), starting from 7 weeks of age. ITT (insulin 0.5 U/kg of body weight) was conducted after 8 weeks of standard diet feeding (B). $n = 5-6$ mice per group. WT mice are represented by white circles with solid dash, $GIP^{gfp/+}$ mice by black squares, and $GIP^{gfp/gfp}$ mice by gray triangles. * $p < 0.05$ $GIP^{gfp/gfp}$ vs WT.

Table 1

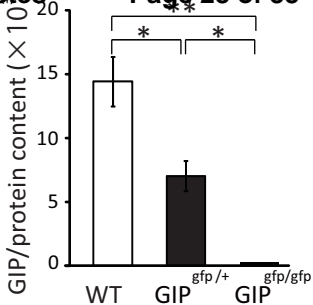
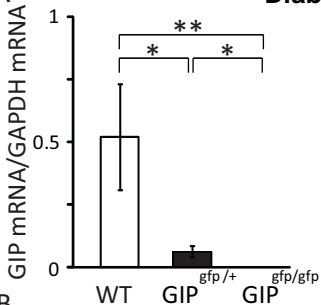
Phenotype comparison of GIP-GFP KI mice and GIPRKO mice

Genotype/ Phenotype	WT	GIP^{gfp/+}	GIP^{gfp/gfp}	GIPRKO^{7,13}
<i>Standard chow feeding</i>				
GIP secretion		↓ (~50%)	absent	↑
Glucose tolerance		impaired	impaired	impaired
Bone volume		↔	↓	↓
<i>High fat diet feeding</i>				
	WT HFD	GIP^{gfp/+} HFD	GIP^{gfp/gfp} HFD	GIPRKO HFD^{6,12,29}
Glucose tolerance		↔	↔	impaired
Body weight		↓	↓↓	↓↓
Fat mass		↓	↓↓	↓↓
Insulin sensitivity		↑	↑↑	↑↑

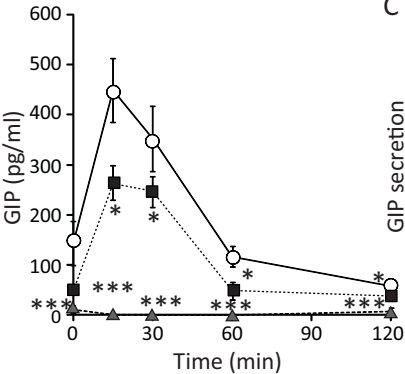
Standard chow feeding data are relative to WT; high fat diet feeding data are relative to WT HFD.

Symbols: “↔”: no changes; “↓”: decreased; “↓↓”: highly decreased; “↑”: increased; “↑↑”: highly increased. Numbers shown in superscript indicate the corresponding articles listed in *References*.

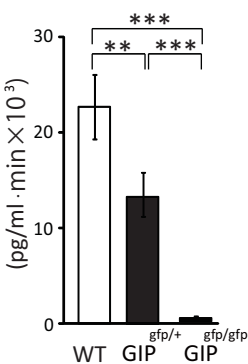
A

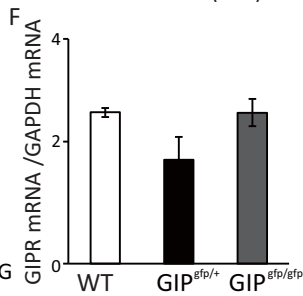
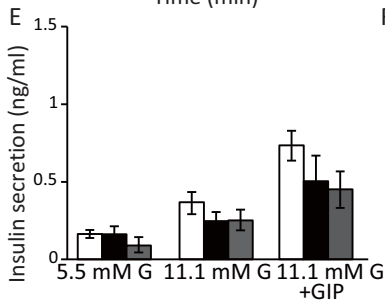
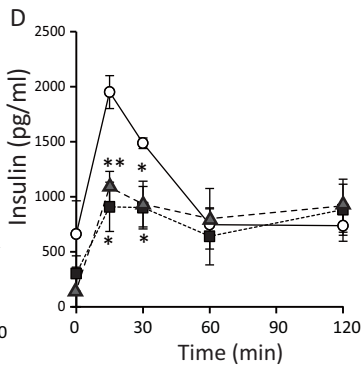
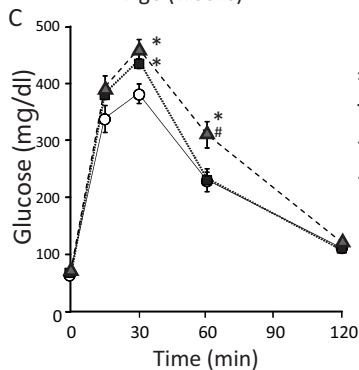
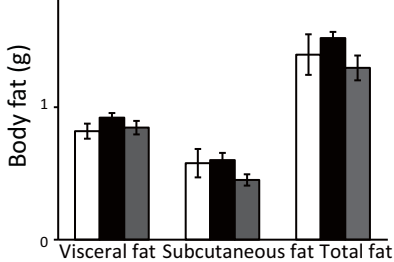
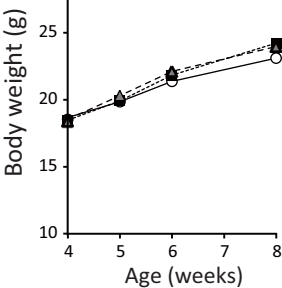


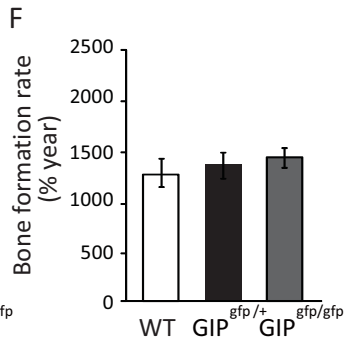
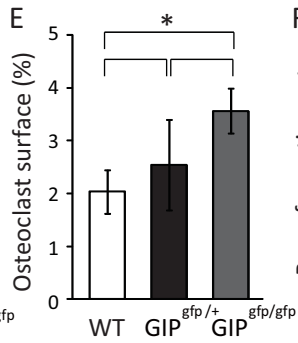
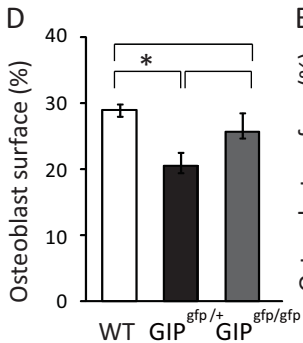
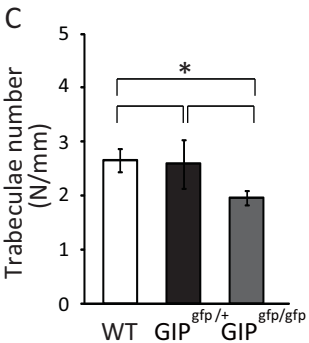
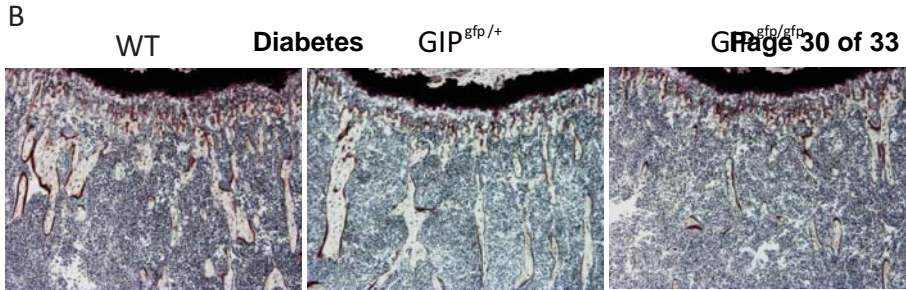
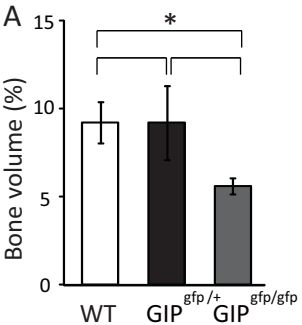
B

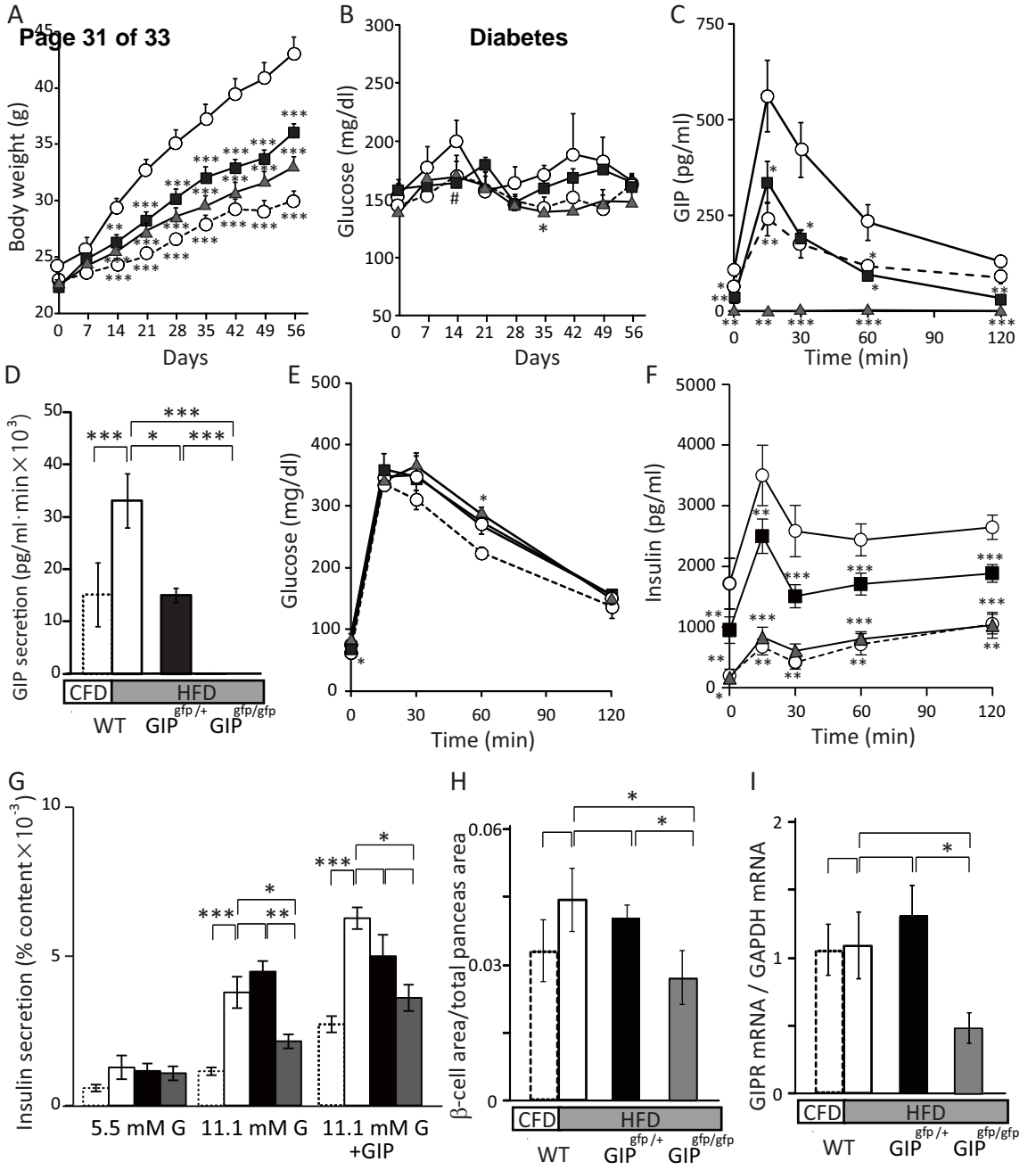


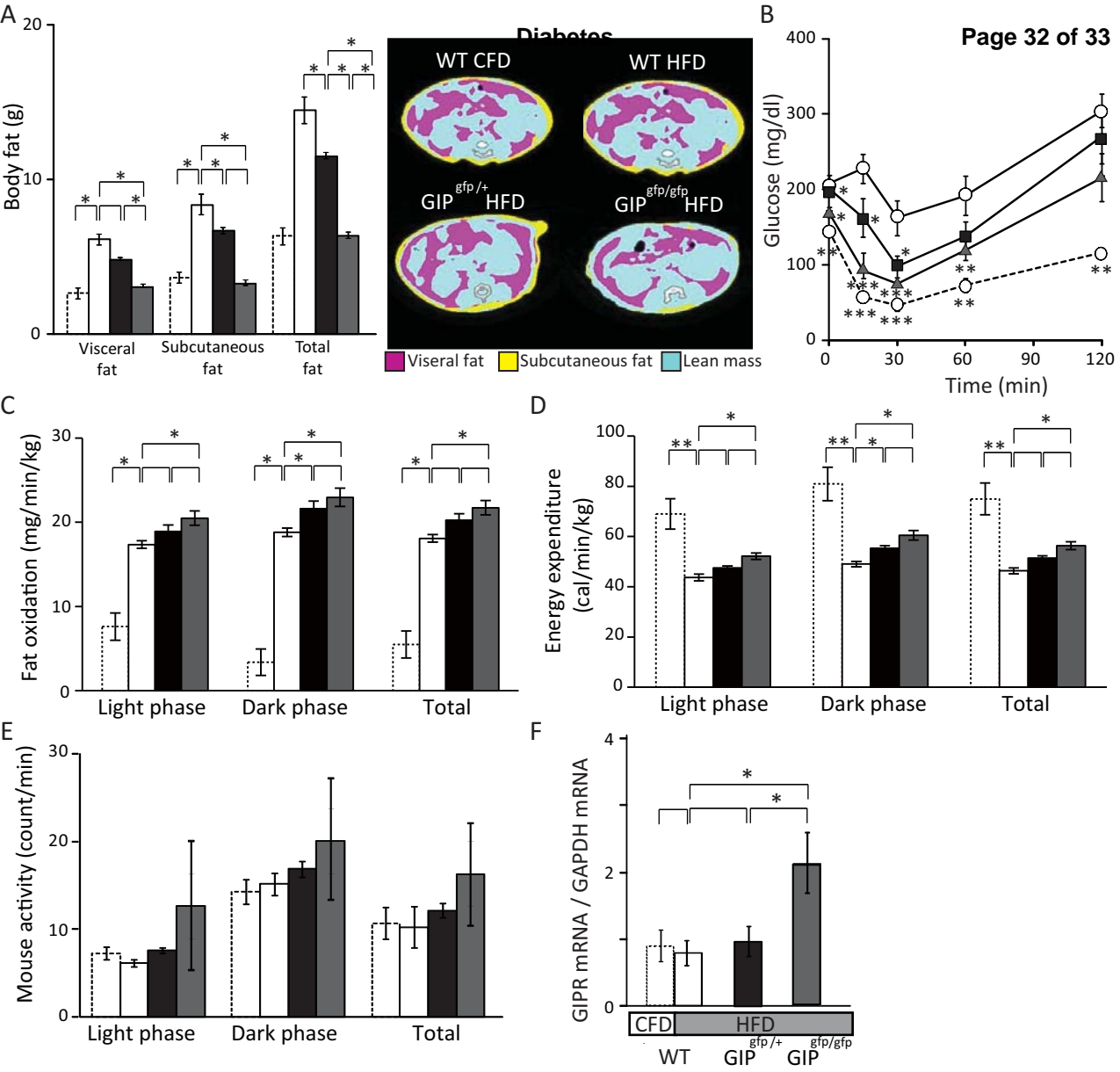
C





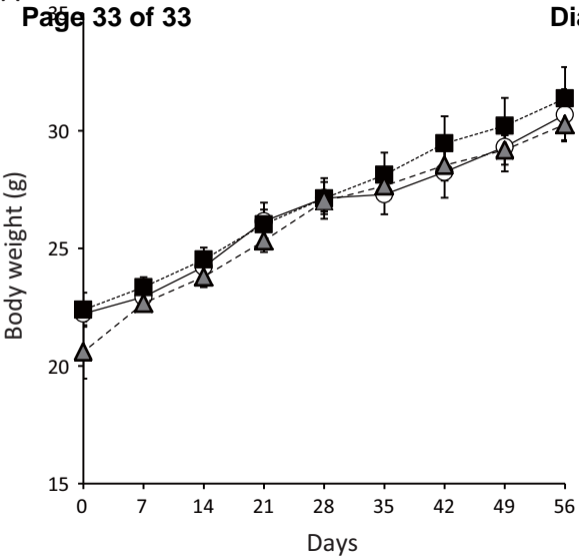






A

Page 33 of 33



B

Diabetes

